Research paper

Evidence for water-permeable channels in auditory hair cells in the leopard frog

Mia E. Miller [c,1], Arian K. Nasiri [a,1], Peyman O. Farhangi [a], Nasser A. Farahbakhsh [a], Ivan A. Lopez [c], Peter M. Narins [a,b,d], Dwayne D. Simmons [a,d,*]

[a] Department of Integrative Biology and Physiology, 610 Charles E. Young Drive East, University of California, Los Angeles, CA 90095-7239, USA
[b] Department of Ecology and Evolutionary Biology, 621 Charles E. Young Drive South, University of California, Los Angeles, CA 90095-1606, USA
[c] Department of Head and Neck Surgery, David Geffen School of Medicine, University of California, Los Angeles, CA 90995-1624, USA
[d] Brain Research Institute, University of California, Los Angeles, CA 90095-1761, USA

ARTICLE INFO

ABSTRACT

Auditory hair cells in the amphibian papilla (APHCs) of the leopard frog, *Rana pipiens pipiens*, have a significantly higher permeability to water than that observed in mammalian hair cells. The insensitivity of water permeability in frog hair cells to extracellular mercury suggests that an amphibian homologue of the water channel aquaporin-4 (AQP4) may mediate water transport in these cells. Using immuno-cytochemistry, we show that an AQP4-like protein is found in APHCs. Rabbit anti-AQP4 antibody was used in multiple-immunohistochemical staining experiments along with AP hair cell and hair bundle markers in leopard frog and mouse tissue. AQP4 immunoreactivity was found in the basal and apical poles of the APHCs and shows uniform immunoreactivity. This study provides the first identification and localization of an AQP4-like protein in the amphibian inner ear. We also report a more direct measure of hyperosmotically-induced volume changes in APHCs that confirms previous findings. The presence of water channels in anuran APHCs constitutes a novel physiological difference between amphibian and mammalian hair cell structure and function.

1. Introduction

In most cells, transmembrane water permeability and intracellular osmolarity are regulated by one or more types of water channels in the cell membrane. These water or aquaporin (AQP) channels are a part of the Major Intrinsic Protein (MIP) superfamily of transmembrane channel proteins. Thirteen types of aquaporins have been identified in mammals (AQP0–AQP12), some of which conduct only water, such as AQP1, AQP2, AQP4, and AQP5, and others which also transport solutes, such as AQP3, AQP7, AQP9, and AQP10 (Ishibashi et al., 2000; Takata et al., 2004; Ishibashi et al., 2011). Anurans are of special interest in the study of cellular water transport, as their transition from aquatic to terrestrial habitats has required unique adaptations to prevent water loss. As anurans, such as the leopard frog, move from dry land to water and back, their body fluid osmolarity changes drastically (Suzuki and Tanaka, 2009). In anurans, the aquaporin family has some overlap

with mammalian types, including AQP0–AQP5 and AQP7–AQP10; there are also anuran-specific aquaporins, including AQPa1 and AQPa2. The anuran aquaporins are localized to a variety of osmo-regulatory tissues. AQP2 and AQP3 are localized to anuran kidney, AQPa2 and AQP3 to ventral pelvic skin and urinary bladder, AQP3 in epidermis, and AQP3 and AQP5 in skin glands in frogs (Suzuki and Tanaka, 2009). Although AQP4 sequence has been identified in amphibians, the tissue-specific presence of the AQP4 in amphibian organs has not been reported, as yet.

The ionic environment and changes in osmolarity within the inner ear affect its sensitivity of the inner ear to sound. In the anuran inner ear, recent reports indicate that hair cells in the amphibian papilla (AP) have extremely high permeability to water, making these cells less vulnerable to inadvertent shape changes and thus loss of function and cell death (Farahbakhsh et al., 2011). AP hair cells change their cell volume in response to hyper- and hypo-osmotic media and these osmolarity-induced changes are insensitive to mercury. Additionally, AP hair cells possess a calcium–calmodulin-dependent slow motility mechanism, which is temporarily accompanied by volume change (Farahbakhsh and Narins, 2006, 2008). The ability of amphibian hair cells to change their volume in an iso-osmotic medium suggests that they may have mechanisms for transporting solutes and water across the cell membrane.

---

* Corresponding author. Department of Integrative Biology and Physiology, 610 Charles E. Young Drive East, University of California, Los Angeles, CA 90095-1606, USA. Tel.: +1 310 794 1228.
E-mail address: dd.simmons@ucla.edu (D.D. Simmons).
[1] Mia Miller and Arian Nasiri are co-first authors.

Having the appropriate permeability to water and ions is most likely a key step in the transduction process in the amphibian inner ear. Previous physiological studies have suggested that AP hair cells have high water permeability and are resistant to inhibition by mercury (Farahbakhsh et al., 2011). To date, AP04 is the only known aquaporin with such permeability properties (Beitz et al., 2003). Therefore, we hypothesized that an AQP4-like protein could be a potential water channel expressed in the plasma membrane of AP hair cells and investigated the presence of AQP4 or its homologue in anuran AP hair cells. In this report we provide the first immuno-cytochemical evidence for the presence of AQP4 in frog AP hair cells. We also further confirm the previously reported ability of AP hair cells to regulate their volume in a hypertonic environment (Farahbakhsh et al., 2011).

2. Methods

2.1. Animals

Adult northern leopard frogs (*Rana pipiens pipiens*) and adult C57Bl/6 mice were used. In all cases, frogs were pithed and then decapitated. Adult mice were given lethal injections of sodium pentobarbital (Nembutal) and then decapitated. All experimental procedures were approved by the Chancellor's Animal's Research Committee and conducted according to the guidelines for Animal Research at UCLA.

2.2. Immunocytochemistry and Western blots

For immunocytochemical labeling experiments in *Rana pipiens pipiens*, we used sectioned AP, whole AP organs and dissociated AP hair cells (APHCs). For sectioned or whole AP organs, papillae were microdissected and fixed in 4% paraformaldehyde for 30 min and 2% paraformaldehyde in 0.02 M phosphate buffer (frog phosphate buffer solution or FPBS) for 1 h. For sectioning, each AP organ was embedded in 0.75% gelatin with 2.5% agarose and sectioned from 100 μm to 150 μm using a Vibratome. Dissociated APHCs (see below) were allowed to adhere to a glass coverslip and then fixed in 2% paraformaldehyde in FPBS for 1 h. Tissues and cells were rinsed in FPBS.

AP tissues and dissociated cells were permeabilized in 1% Triton for 30 min and then washed several times in FPBS. They were then blocked for 1 h with 1–2% BSA. Primary antibody incubation proceeded for 4 h for dissociated cells and overnight for sections and whole organs. Primary antibodies used were: rabbit anti-AQP4 (1:200 dilution, sc-20812, Santa Cruz), goat anti-α-parvalbumin (1:400 dilution, PVG-214, Swant), and rabbit anti-GAD67 (1:1000 dilution, kindly provided by Dr. N.J. Tillakaratne). The rabbit anti-AQP4 (sc-20812) antibody cross reacts with human and rat inner ear, cerebellum and kidney. Positive and negative controls were previously tested by Lopez et al. (2007). All incubations were performed at room temperature unless otherwise stated. AP tissues and cells were washed several times between primary and secondary antibody incubations in FPBS. Secondary antibody incubations with Northern Lights (R&D Systems) and/or Alexa (Invitrogen) secondary antibodies were performed for two hours in BSA with 10% normal donkey serum (NDS). After several washes, tissues and cells were cover slipped using Confocal Matrix mounting media.

Adult mice were perfused with 4% paraformaldehyde in 0.2 M phosphate buffer (PBS) and decapitated. The brain was removed and fixed overnight in 4% paraformaldehyde in PBS. The temporal bones were removed and fixed overnight in the same solution. Cochleae were decalcified for several days with 14% EDTA in PBS (pH 7.2). Once the cochleae were fully decalcified, both the cochlea and brain were embedded in 0.75% gelatin with 2.5% agarose and sectioned to 100 μm thickness. The sections were permeabilized with 1% Triton for 1 h, or 0.5% Triton for 30 min, and then rinsed several times in PBS. Sections were blocked with 0.3% Triton with 3% NDS in PBS for 1 h. Primary antibodies were incubated overnight in block solution. Sections were rinsed between primary and secondary antibodies several times in PBS. Secondary antibody incubations were with Northern Lights antibodies for 2 h. Sections were then rinsed and mounted.

For Western blots, we used a rabbit AQP4 primary antibody (dilution 1:1000; Santa Cruz) and HRP-goat anti-rabbit IgG secondary antibody (dilution 1:25,000; Invitrogen). Tissue samples from brain and kidney were frozen in liquid N_2, pulverized to a fine powder, and then resuspended in Laemmle buffer (containing 1% SDS, 31.25 mM Tris, 5% glycerol and 200 mM 2-mercaptoethanol). Equal amounts of homogenates were separated on a 10% SDS-PAGE. Proteins were transferred to PVDF membranes (Bio-Rad), and blocked for 2 h with 5% BSA in TBS containing 0.05% Tween-20 (TBS-T). Membranes were incubated with primary antisera overnight at 4 °C and followed by appropriate washes with TBS-T. Blots were incubated for 2 h in secondary antisera. Membranes were subsequently washed with TBS-T and developed with Supersignal ECL reagent (Pierce).

2.3. Confocal microscopy

Labeled organs were imaged with a confocal microscope (Zeiss LSM 5) attached to an upright microscope (Zeiss, AxioImager). The confocal microscope is equipped with single-photon [Argon (488, 514 nm), HeNe (543 nm) and Red Diode (633 nm)] lasers. The same acquisition parameters were used for all control and experimental scans. Image processing was performed with Volocity software.

2.4. Dissociation of hair cells

Amphibian papillae were dissected out of pithed leopard frogs, and hair cells were gently scraped free from trypsin-treated APs in the recording chamber as described previously (Farahbakhsh and Narins, 2006, 2008). The dissociated APHCs adhered to the floor of the chamber and were perfused for 3 min with a solution composed of (in mM): NaCl, 110; KCl, 2; CaCl$_2$, 2; MgCl$_2$, 0.8; D-glucose, 3; HEPES, 10 (hereafter referred to as the AP solution). The pH was titrated to 7.2 with NaOH. Osmolarity was adjusted to 223–227 mosmol l^{-1} with a vapor pressure osmometer (Vescor, model 5520, Logan, UT).

2.5. The chamber and experimental setup

The recording chamber for physiological experiments consisted of a modified plastic petri dish with a glass cover slip as its bottom, and a plastic insert to reduce its effective volume to 500 μl. Dissociated AP hair cells were loaded with the fluorescent dye, X-Rhod-1 by adding 2 μl of the mixture containing 50 μg X-Rhod-1-AM, 10 μl DMSO and 90 μl AP solution to the chamber filled with the AP solution. After 40 min, the cells were washed with the AP solution alone for 3 min to remove the extracellular dye. During the recording, the cells remained bathed in the AP solution. However, to avoid perturbation and to improve the image registration, perfusion was stopped. To induce shape change in hair cells, a 2-μl volume of a concentrated sucrose solution was injected into the chamber through a tapered pipette with a 0.38-mm-diameter orifice, in 100 ms. The injection pipette was positioned 5 mm from, and pointed toward, hair cells adhered to the center of chamber's floor. The peak sucrose concentration in the vicinity of the hair cells was estimated to be 8% of that in the pipette, while the final sucrose
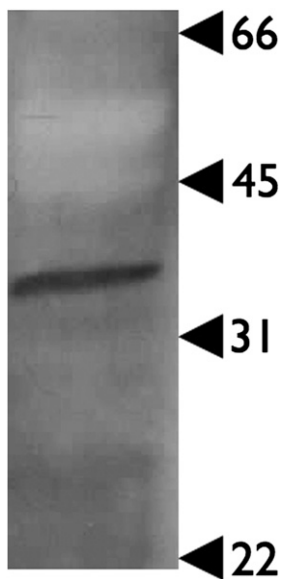
Fig. 1. Western blot detects AQP4 in brain homogenates from *Rana pipiens pipiens*. The rabbit polyclonal antibody against human AQP4 reveals a unique protein band with an estimated molecular weight near 34 kDa.

concentration in the chamber was 0.4% of the injected concentration. The assumptions underlying these estimates, and the detail and justification for other measurement methodologies utilized here, are reported in a previous study (Farahbakhsh et al., 2011).

2.6. Fluorescence imaging

The recording chamber containing dissociated hair cells was placed on the stage of an inverted microscope (Zeiss, Axio-observer AX10), equipped with the hardware and software required for confocal microscopy by Perkin Elmer (Ultra View ERS and Improvision). Hair cells loaded with X-Rhod-1 fluorescent dye were excited at 550 nm, and the emitted fluorescence light at 600 nm was recorded. A stack of 41 horizontal optical sections spaced 0.5 μm along the z-axis, each covering an image area of 63.2 by 63.2 μm (512 × 512 pixels) was scanned at 3-s intervals. For off-line analysis, 3-D images of hair cells were reconstructed from these scanned sections using software (Volocity, Improvision/Perkin–Elmer). This software calculated the average light intensity, cell surface area and volume. It should be emphasized that even though X-Rhod-1 is a Ca^{2+}-sensitive fluorescent dye it was solely used here for its bright fluorescence that assisted in the measurement of the physical properties — length, diameter, surface area and volume — of APHCs. No attempt was made to calibrate its Ca^{2+} sensitivity, or
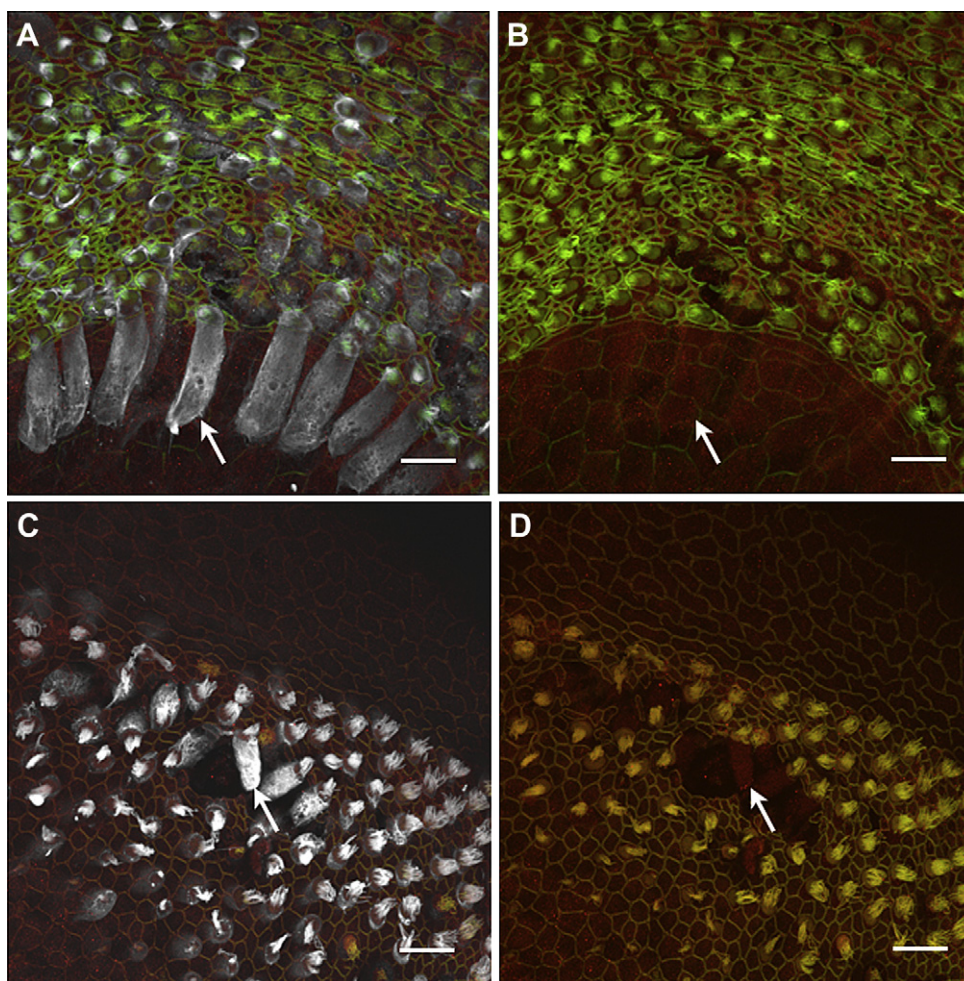

Fig. 2. AQP4 immunoreactivity is present in AP whole mounts. For all images, AQP4 is labeled in red, α-parvalbumin in white, and phalloidin in green. The first image (A and C) of each pair shows all three channels, while the second image (B and D) does not show α-parvalbumin on the white channel, to better compare intensity of AQP4 immunoreactivity. In panels A and B, AQP4 labels hair cells in the rostral AP. In panels C and D, AQP4 labels hair cells in the caudal AP. The arrows indicate individual hair cells labeled across image pairs. [For interpretation of the references to colour in this figure legend, the reader is referred to the web version of this article.]

to use it as a Ca^{2+} indicator. Nor did we try to interpret the increase in the intensity of its florescence during osmotically induced shrinkage as a quantitative (inverse) indicator of volume change per se.

3. Results

3.1. Characterization of AQP4

A previous report suggested that the high water permeability in amphibian papilla hair cells (APHCs) was insensitive to mercury (Farahbakhsh et al., 2011). Because of its known mercurial insensitivity, we investigated whether water channels similar to AQP4 might be present in the amphibian inner ear. First to verify that our antisera could detect an AQP4-like protein in amphibian tissues, we performed Western blot analysis on brain and kidney homogenates from adult *Rana pipiens pipiens* and mice. We screened several mammalian antisera against AQP4 that gave rise to a single band in mouse but multiple bands in the frog (data not shown). The AQP4 antisera we report here was raised against amino acids 244–323 near the C-terminus of human AQP4 and recognizes a single protein band in the mouse kidney of the expected molecular weight around 34 kDa (data not shown). This AQP4 antibody cross reacts with a single protein of similar molecular weight in the amphibian brain (Fig. 1), demonstrating that an AQP4-like protein is indeed present in amphibian tissues.

3.2. AQP4 channel-like immunoreactivity

Using the AQP4 antisera screened by Western blot analysis, we examined the expression and differential spatial distribution of the AQP4 immunoreactivity in the AP using whole organs and Vibratome sections (100 μm thickness). In all immunocytochemical experiments, we also used α-parvalbumin antisera to label hair cell bodies and phalloidin staining to label hair bundles. We observed AQP4 immunoreactivity in APHCs found in both rostral and caudal regions of the AP (Fig. 2). In cross-sections, AQP4 immunoreactivity preferentially localized to the apical and basal poles of the hair cell. The apical pole localization generally was associated with labeling near or on the hair bundle (Fig. 2D). Frequently, the AQP4 immunoreactivity had a punctate appearance within APHCs. There were some regional differences in AQP4 immunoreactivity as well. Hair cells in caudal regions of the AP more often demonstrated labeling near or at the hair bundle, whereas APHCs along the medial border labeled more robustly than APHCs along the lateral edges. Thus, we conclude that AQP4 immunoreactivity is present across the entire sensory epithelium.

In addition to APHCs, AQP4 immunoreactivity was also present in the nerve fibers innervating the AP but not in supporting cells below APHCs within the epithelium (Fig. 3A). The AQP4 immunoreactivity was found in the distal portions of the innervating nerve fibers. However, AQP4 immunoreactivity was absent medially as the fibers entered the sensory epithelium. This pattern of labeling is consistent with that the labeling present in the glial cells
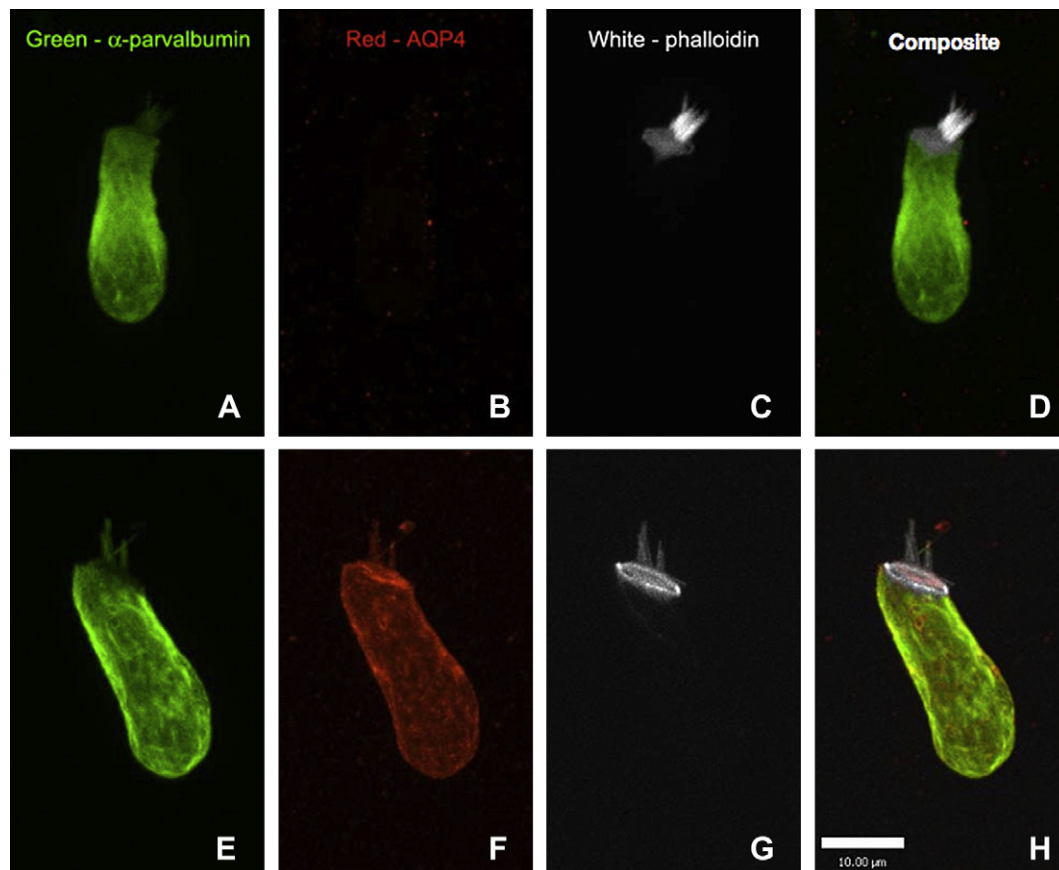

Fig. 3. Aquaporin immunoreactivity is present in isolated AP hair cells. In the top panel (A–D), α-parvalbumin is labeled on the green channel (A) and phalloidin is labeled on the white channel (C). The red channel (B) shows the secondary antibody control for AQP4 (i.e., no primary antibody). A composite image of all three channels is also shown (D). In the bottom panel (E, F), α-parvalbumin is green (E), AQP4 is red (F) and phalloidin is white (G). The AQP4 immunoreactivity shows preferential membrane labeling near the cuticular plate and along the lateral membrane. A composite image of all three channels is also shown (H). The scale bar (H) is the same for all panels. [For interpretation of the references to colour in this figure legend, the reader is referred to the web version of this article.]

surrounding the neurons. Additional control experiments for AQP4 were carried out in mouse brain and cochlea. In the mouse brain, AQP4 immunoreactivity was identified lining the ventricles (Fig. 3B). In the cochlea, AQP4 was found in spiral ganglion cells and supporting cells, but not in inner or outer hair cells (Fig. 3C).

To explore the intracellular localization of the AQP4 localization, APHCs were isolated as for hyperosmotic challenge experiments below, fixed, and labeled for APQ4, α-parvalbumin and phalloidin (Fig. 4). A secondary antibody control was performed in which no AQP4 antibody was used. In all such cases, there was no AQP4 labeling (Fig. 4B). In APHCs isolated from caudal regions, AQP4

immunoreactivity was identified throughout the APHC cytoplasm with a preference for the lateral membrane and the apical region near the cuticular plate (Fig. 4F). AQP4 labeling was also seen in the hair bundle. We conclude that APQ4 immunoreactivity is associated with specific labeling of APHCs.

3.3. Confocal imaging of hair cell shape changes

The hypothesis that APHCs may have an APQ4-like water channel came from a previous study based on indirect measurement of volume changes that show an osmotic permeability much larger than that expected from lipid bilayers or measured from mammalian outer hair cells (Farahbakhsh et al., 2011). Using confocal microscopy to give a more direct measure of hyperosmotically-induced volume changes, we corroborated these previous estimates of permeability coefficients in three APHCs. Fig. 5 shows the time course of changes in the X-Rhod-1 fluorescence (panel A), length (panel B) and volume (panel C) for a single, 35-μm-long dissociated APHC. Transient changes in response to injection of 2 μl of 0.25 and 1.5 M sucrose are observed in all measured parameters. Injection of 0.25 M sucrose produced a 4.6% increase in the fluorescence intensity and a 1.1% decrease in the length. Volume measurement with Volocity software indicated a 4% decrease in the volume, with a time constant of 4.5 s. From the rates of volume change at the onset of response, we estimated an osmotic permeability coefficient of 0.8×10^{-2} cm/s for this cell (for the estimation method, see Farahbakhsh et al., 2011). The response to the second larger hyperosmotic shock (2 μl of 1.5 M sucrose) showed a 63% increase in the fluorescence intensity, and an 18% decrease in the length. Volume decrease in response to the injection of 1.5 M sucrose was 45.6% in 6 s (the time constant of this volume decrease was 3.5 s). The corresponding osmotic permeability coefficient was 2.3×10^{-2} cm/s.

Fig. 6 shows the confocal images of this hair cell before (panel A) and during (panels B–D) the response to the larger hyperosmotic shock at the times indicated by downward arrows in Fig. 5. Similar results were obtained by recording shape changes in two additional mediorostral hair cells (40 and 51 μm in length) in response to the injection of 2 μl of 250 μM and 1.5 M sucrose into the chamber. The
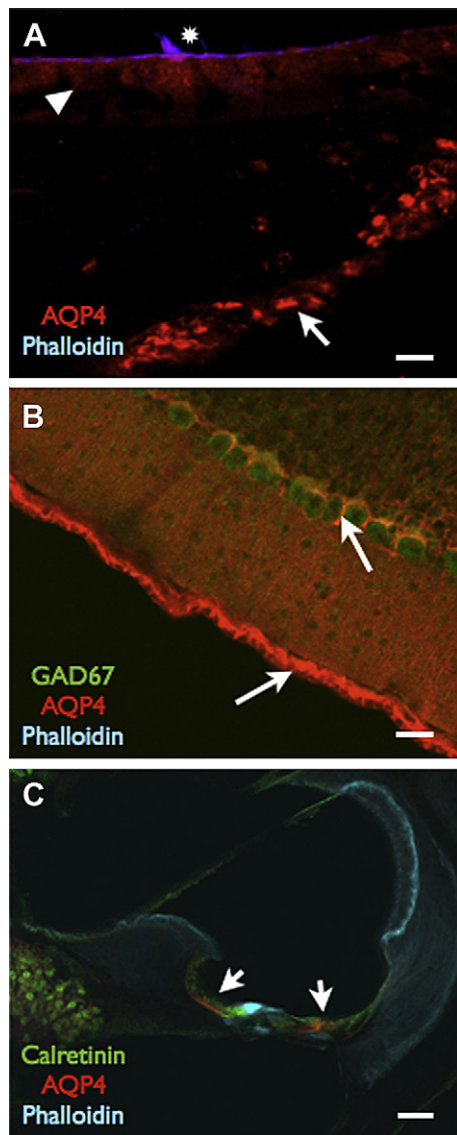

Fig. 4. Aquaporin immunoreactivity found in the frog AP and mouse brain and cochlea. A. A cross-section of the AP shows AQP4 immunoreactivity (red) in the distal processes of the nerve fibers approaching the sensory epithelium and in APHCs (arrowhead). Phalloidin (blue) labels the cuticular plate and hair bundle. A single hair bundle (asterisk) shows labeling for both phalloidin and AQP4. B. AQP4 is labeled on the red channel and shows robust labeling in the cells surrounding the ventricles of mouse brain tissue. Purkinje cells are labeled with GAD67 in green. C. In this cross section of a basal cochlear turn, AQP4 (red) labels supporting cells within the organ of Corti, and is not apparent in inner or outer hair cells in the mouse cochlea. Calretinin is labeled on the green channel, and phalloidin is labeled in cyan. Scale bars are 10 μm (A), 20 μm (B), and 40 μm (C). [For interpretation of the references to colour in this figure legend, the reader is referred to the web version of this article.]
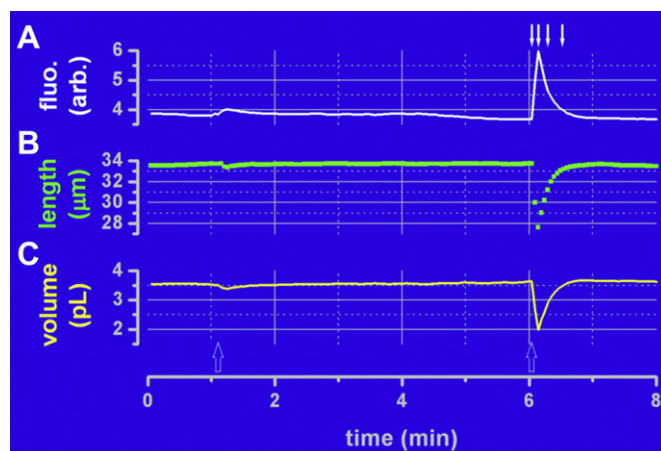

Fig. 5. A: The time course of the average fluorescence intensity emitted from a cell loaded with X-Rhod-1 fluorescent dye and excited at 550 nm. The white arrows show the time points represented by the images in Fig. 6. B: The time course of changes in the cell's length (in μm) measured every 3 s (green solid squares). C: The time course of changes in the cell's volume (in pL = 1000 μm^3) measured using commercial software, Volocity (yellow line). The times at which 2 μl of 0.25 M sucrose (left open arrow), and 2 μl of 1.5 M sucrose (right open arrow) were injected are indicated. [For interpretation of the references to colour in this figure legend, the reader is referred to the web version of this article.]
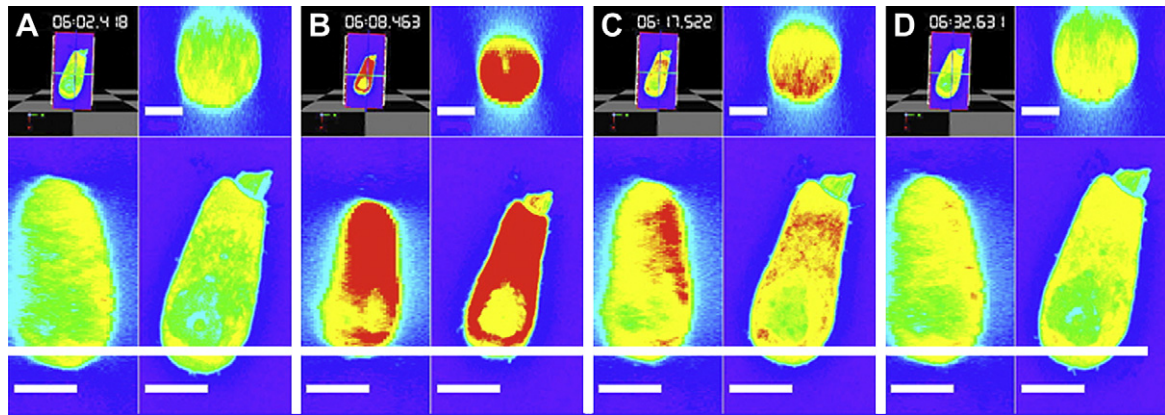
Fig. 6. Transient hyperosmotically-induced shape changes in a single hair cell dissociated from the caudal region of the leopard frog's amphibian papilla. Four panels showing horizontal (lower right quadrant), and vertical (lower left and upper right quadrants) cross-sections of the cell recorded with the confocal microscope, before (A) (362.4 s after the start of recording) and after (B–D) (at 368.5, 377.5 and 392.6 s) injection of 2 μl of 1.5 M sucrose into the 500-μl-recording chamber (the position of the vertical cross-sections are shown in the upper left quadrant; see Methods for the experimental setup). Horizontal (white) scale bars in the upper quadrants represent 6 μm; scale bars in the lower quadrants show 10 μm.

estimates of the osmotic permeability coefficient for these three cells (Table 1) are within the range reported recently (Farahbakhsh et al., 2011).

4. Discussion

In the present study, we provide the first demonstration of AQP4, or a water channel with sufficient homology to be labeled by an anti-AQP4 antibody, in auditory hair cells of the anuran inner ear. This study also provides additional physiological evidence for the presence of water channels using confocal microscopy confirming previous estimates of osmotic permeability coefficients. Recently, AQP4 was also reported in non-auditory hair cells of the adult zebra fish (Zichichi et al., 2011). Therefore, an AQP4-like water channel may be commonly expressed in non-mammalian hair cells. It is possible that anurans and fish maintain functional water channels in hair cells as a response to the unique requirements of their environments.

Our Western blot and control experiments support the specificity of the anti-AQP4 antibody used in this study. As previous studies of APQ4 have shown, Western blot analysis shows a specific protein band with an estimate molecular weight near 34 kDa. Using this antibody, immunohistochemical control experiments also find prominent APQ4 labeling in mouse brain tissue, particularly lining the ventricles, and in supporting cells of the inner ear, but not in inner or outer hair cells as previous studies have demonstrated (Mhatre et al., 2002; Lopez et al., 2007). In the AP, AQP4 immunoreactivity was restricted mostly to hair cells and nerve fibers, suggesting a rather defined localization.

Table 1
Volume decrease time constants ($\tau_{v\ dec}$) and estimated osmotic permeability coefficients (Pf) of three amphibian papillar hair cells.

Hair cell length (μm)	250 mM sucrose		1.5 M sucrose	
	$\tau_{v\ dec}$ (s)	P_f ($\times 10^{-2}$ cm/s)	$\tau_{v\ dec}$ (s)	P_f ($\times 10^{-2}$ cm/s)
35	4.5	0.8	3.5	2.3
40	14.3	2.1	3.5	1.8
51	13.8	2.0	8.9	1.1
Mean ± SE	10.9 ± 3.2	1.6 ± 0.4	5.3 ± 1.8	1.7 ± 0.3

See Farahbakhsh et al., 2011, for detailed description of methods used for hair cell volume measurement and osmotic permeability coefficient estimation.

Although some aquaporins have been identified in human cochlear and vestibular cell types through immunohistochemical experiments, no named aquaporin has been identified in mammalian hair cells (Lopez et al., 2007). Water-permeable channels have been identified in the mammalian inner ear, in the endolymphatic duct and sac, stria vascularis, and spiral ligament, in addition to the supporting cells (Stankovic et al., 1995; Huang et al., 2002; Merves et al., 2003; Sawada et al., 2003; Zhong and Liu, 2003). AQP1 is found in fibrocytes of the spiral ligament and the sub-basilar tympanic cells; AQP4 is found in the outer sulcus cells, Hensen's cells, and Claudius' cells; AQP6 in the apical portion of the interdental cells in the spiral limbus.

Although AQP4 is expressed in anurans and might possibly be one of the oldest water channels in vertebrates, there have been few studies of its location and function outside of oocytes (Nishimoto et al., 2007; Suzuki and Tanaka, 2009). In mammals, AQP4 is also expressed in astroglial cells at the blood–brain barrier and spinal cord, kidney collecting duct, glandular epithelia, airways, skeletal muscle, stomach and retina (Gomes et al., 2009). The high expression of AQP4 in brain glial cells, particularly in the end-feet of astrocytes, coincides with its colocalization with inward rectifier K^+ channels (Nagelhus et al., 2004). Mice with a targeted deletion of AQP4, have both impaired hearing and in the brain, altered cerebral water balance with protection from brain edema (Manley et al., 2000; Li and Verkman, 2001). These studies have suggested that AQP4 is a critical component of an integrated water and K^+ homeostasis required for the maintenance of neuronal excitability (Takumi et al., 1998; Manley et al., 2000). In the mammalian inner ear, AQP4 is believed to play a role facilitating the flow of K^+ ions in the organ of Corti and lateral wall supporting cells by allowing swift osmolarity changes in supporting epithelial cells via rapid water flux (Li and Verkman, 2001; Mhatre et al., 2002).

Our immunocytochemical labeling experiments confirm the distinction between amphibian hair cells and mammalian hair cells. In a recent study of amphibian auditory hair cells, it was argued that the rather large osmotic permeability coefficient and relative insensitivity to mercurial inhibition are most consistent with the expression of AQP4 in order to account for osmotically induced volume changes (Farahbakhsh et al., 2011). In the present study, we used the same methodology as in Farahbakhsh et al. (2011), including a) an injection pipette capable of rapidly exposing hair cells to osmotic challenge without producing mechanical artifacts (Zhi et al., 2007), and b) the use of only the

volume change at the onset of osmolarity change, in order to estimate the permeability coefficient for water. Our estimates of the osmotic permeability coefficients are within the range previously reported for APHCs hair cells (Farahbakhsh et al., 2011), and are comparable with the osmotic permeability coefficient of epithelial cells in a number of species (Finkelstein, 1976; Verkman, 1989), suggesting that APHCs express water channels with high permeabilities. However, these estimates of the osmotic permeability coefficient in amphibian hair cells are more than an order of magnitude larger than that reported for mammalian outer hair cells (Ratnanather et al., 1996), indicating that the latter cell types may not express functional water channels in their plasma membrane (Zhi et al., 2007). The presence of an AQP4-like channel in the anuran AP hair cell may constitute an important physiological difference between amphibian and mammalian hair cells, until a mammalian counterpart is identified. To date, the presence of water channels in mammalian outer hair cells has not been unambiguously confirmed.

References

Beitz, E., Zenner, H.P., Schultz, J.E., 2003. Aquaporin-mediated fluid regulation in the inner ear. Cell. Mol. Neurobiol. 23, 315–329.

Farahbakhsh, N.A., Narins, P.M., 2006. Slow motility in hair cells of the frog amphibian papilla: Ca^{2+}-dependent shape changes. Hear. Res. 212, 140–159.

Farahbakhsh, N.A., Narins, P.M., 2008. Slow motility in hair cells of the frog amphibian papilla: myosin light chain-mediated shape change. Hear. Res. 241, 7–17.

Farahbakhsh, N.A., Zelaya, J.E., Narins, P.M., 2011. Osmotic properties of auditory hair cells in the leopard frog: evidence for water-permeable channels. Hear. Res. 272, 69–84.

Finkelstein, A., 1976. Nature of the water permeability increase induced by antidiuretic hormone (ADH) in toad urinary bladder and related tissues. J. Gen. Physiol. 68, 137–143.

Gomes, D., Agasse, A., Thiebaud, P., Delrot, S., Geros, H., Chaumont, F., 2009. Aquaporins are multifunctional water and solute transporters highly divergent in living organisms. Biochim. Biophys. Acta 1788, 1213–1228.

Huang, D., Chen, P., Chen, S., Nagura, M., Lim, D.J., Lin, X., 2002. Expression patterns of aquaporins in the inner ear: evidence for concerted actions of multiple types of aquaporins to facilitate water transport in the cochlea. Hear. Res. 165, 85–95.

Ishibashi, K., Kuwahara, M., Sasaki, S., 2000. Molecular biology of aquaporins. Rev. Physiol. Biochem. Pharmacol. 141, 1–32.

Ishibashi, K., Kondo, S., Hara, S., Morishita, Y., 2011. The evolutionary aspects of aquaporin family. Am. J. Physiol. Regul. Integr. Comp. Physiol. 300, R566–R576.

Li, J., Verkman, A.S., 2001. Impaired hearing in mice lacking aquaporin-4 water channels. J. Biol. Chem. 276, 31233–31237.

Lopez, I.A., Ishiyama, G., Lee, M., Baloh, R.W., Ishiyama, A., 2007. Immunohistochemical localization of aquaporins in the human inner ear. Cell. Tissue Res. 328, 453–460.

Manley, G.T., Fujimura, M., Ma, T., Noshita, N., Filiz, F., Bollen, A.W., Chan, P., Verkman, A.S., 2000. Aquaporin-4 deletion in mice reduces brain edema after acute water intoxication and ischemic stroke. Nat. Med. 6, 159–163.

Merves, M., Krane, C.M., Dou, H., Greinwald, J.H., Menon, A.G., Choo, D., 2003. Expression of aquaporin 1 and 5 in the developing mouse inner ear and audiovestibular assessment of an Aqp5 null mutant. J. Assoc. Res. Otolaryngol. 4, 264–275.

Mhatre, A.N., Stern, R.E., Li, J., Lalwani, A.K., 2002. Aquaporin 4 expression in the mammalian inner ear and its role in hearing. Biochem. Biophys. Res. Commun. 297, 987–996.

Nagelhus, E.A., Mathiisen, T.M., Ottersen, O.P., 2004. Aquaporin-4 in the central nervous system: cellular and subcellular distribution and coexpression with KIR4.1. Neuroscience 129, 905–913.

Nishimoto, G., Sasaki, G., Yaoita, E., Nameta, M., Li, H., Furuse, K., Fujinaka, H., Yoshida, Y., Mitsudome, A., Yamamoto, T., 2007. Molecular characterization of water-selective AQP (EbAQP4) in hagfish: insight into ancestral origin of AQP4. Am. J. Physiol. Regul. Integr. Comp. Physiol. 292, R644–R651.

Ratnanather, J.T., Zhi, M., Brownell, W.E., Popel, A.S., 1996. Measurements and a model of the outer hair cell hydraulic conductivity. Hear. Res. 96, 33–40.

Sawada, S., Takeda, T., Kitano, H., Takeuchi, S., Okada, T., Ando, M., Suzuki, M., Kakigi, A., 2003. Aquaporin-1 (AQP1) is expressed in the stria vascularis of rat cochlea. Hear. Res. 181, 15–19.

Stankovic, K.M., Adams, J.C., Brown, D., 1995. Immunolocalization of aquaporin CHIP in the guinea pig inner ear. Am. J. Physiol. 269, C1450–C1456.

Suzuki, M., Tanaka, S., 2009. Molecular and cellular regulation of water homeostasis in anuran amphibians by aquaporins. Comp. Biochem. Physiol. A Mol. Integr. Physiol. 153, 231–241.

Takata, K., Matsuzaki, T., Tajika, Y., 2004. Aquaporins: water channel proteins of the cell membrane. Prog. Histochem. Cytochem. 39, 1–83.

Takumi, Y., Nagelhus, E.A., Eidet, J., Matsubara, A., Usami, S., Shinkawa, H., Nielsen, S., Ottersen, O.P., 1998. Select types of supporting cell in the inner ear express aquaporin-4 water channel protein. Eur. J. Neurosci. 10, 3584–3595.

Verkman, A.S., 1989. Mechanisms and regulation of water permeability in renal epithelia. Am. J. Physiol. 257, C837–C850.

Zhi, M., Ratnanather, J.T., Ceyhan, E., Popel, A.S., Brownell, W.E., 2007. Hypotonic swelling of salicylate-treated cochlear outer hair cells. Hear. Res. 228, 95–104.

Zhong, S.X., Liu, Z.H., 2003. Expression of aquaporins in the cochlea and endolymphatic sac of guinea pig. ORL J. Otorhinolaryngol. Relat. Spec. 65, 284–289.

Zichichi, R., Magnoli, D., Montalbano, G., Laura, R., Vega, J.A., Ciriaco, E., Germana, A., 2011. Aquaporin 4 in the sensory organs of adult zebrafish (Danio rerio). Brain Res. 1384, 23–28.